Structural, morphological and luminescence studies of Fe-doped PbI_2 crystals

Rybak O. V. and Chekaylo M. V.

Lviv Polytechnic National University, 12 S. Bandera Street, Lviv 79013, Ukraine
oksana.v.rybak@lpnu.ua

Received: 31.10.2021

Abstract. We present the results of X-ray diffraction studies for undoped and Fe-doped single crystals of lead iodide in the concentration range 0.01–0.25 at. %. PbI_2 and PbI_2:Fe crystals are obtained by crystallization from a vapour phase in a closed system under over-stoichiometric iodine-vapour pressure. Morphology of the crystals has been analyzed by a scanning electron microscopy. The effect of iron doping on the low-temperature (T = 4.2 K) photoluminescence spectra of lead iodide has been elucidated.

Keywords: lead iodide crystals, iron doping, X-ray diffraction patterns, photoluminescence spectra

UDC: 535.37

1. Introduction

Direct-bandgap layered PbI_2 semiconductor is characterized by large atomic numbers of its constituent elements, high density and high electrical resistance. Due to possibilities for its use in room-temperature ionizing-radiation detectors, this material has deserved great attention of researchers since 1970s [1, 2]. Lead iodide is also utilized in the solar cells based on both inorganic and organic–inorganic lead-halide perovskites, whose energy conversion efficiency exceeds 22% [3–6], as well as in photodetectors and some optoelectronic devices [7–9].

Doping of semiconductors represents a well-known method for purposeful improvement of their material parameters. Introduction of the elements with unfilled 3*d* shell, e.g. iron, into the crystal lattice of PbI_2 enables one to obtain quasi-2D semi-magnetic semiconductors, which represent promising materials for spintronics [10]. In addition to carrier–ion exchange interaction, i.e. interaction among the localized spins of magnetic ions and the spins of current carriers (electrons and/or holes), an ion–ion exchange interaction among the magnetic ions takes place in these semi-magnetic semiconductors.

The largest number of works devoted to the influence of transition-metal dopants on the properties of lead iodide concerns manganese [11, 12]. Nonetheless, there are a few studies reported on Fe-doped PbI_2 single crystals. They refer to the crystals grown from a vapour phase or by a Bridgman–Stockbarger method [13–15], as well as to $Pb_{1-x}Fe_xI_2$ nanoparticles dispersed in polymer matrices [14]. The authors of Ref. [13] have considered the effect of iron impurity on the mass-transfer rate in the PbI_2–I_2 system and the quality of crystals grown during crystallization from the vapour phase in a closed system under over-stoichiometric iodine-vapour pressure. The effect of Fe on the parameters of low-temperature excitonic photoluminescence bands has also been revealed. The work [14] has presented the experimental results found for absorption spectra, photoluminescence and electron paramagnetic resonance of $Pb_{1-x}Fe_xI_2$ nanoparticles dispersed in a matrix of polyvinyl alcohol and in colloidal solutions of nanoparticles.

The purpose of this work is to study the effect of iron dopant on the structure, morphology and low-temperature photoluminescence spectra of the lead iodide crystals grown from the vapour phase in the closed system under the vapour pressure of over-stoichiometric iodine.

2. Experimental

PbI_2 was doped with iron while it was growing from the vapour phase in the closed system under the vapour pressure of over-stoichiometric iodine. This has been done according to the method described in detail in Ref. [13].

The concentration of Fe in the single crystals was determined by an X-ray micro-analyzer "Camebax". The analysis was performed on the Fe-K_α lines at the accelerating voltage 20 kV and the beam current $\approx 10^{-8}$A.

X-ray powder diffraction patterns of the crystals were obtained using a STOE Transmission Diffractometer System STADI P. The following parameters and conditions were used in the X-ray diffraction experiments: Cu-Kα_1 radiation, a curved (111) Ge Johann-type monochromator working on a primary beam, 2θ/ω scanning mode, the angular range 5.0–110.588° 2θ for data collection (with the 0.015° 2θ step), a linear position-sensitive detector with the recording step 0.480° 2θ and the shooting time 260 s, the voltage $U = 40$ kV, the current $I = 30$ mA, and room-temperature ($T = 20$°C) measurement conditions. Analytical indexing of our samples and determination of their space group were performed using an N-TREOR09 device. The crystal structure was refined with a Rietveld method and a FullProf.2k software package (version 5.60), using a pseudo-Voigt profile function and isotropic approximation for the atomic-shift parameters.

Morphological features of our crystals were investigated using optical and scanning electron microscopes.

Low-temperature photoluminescence spectra for the system PbI_2+0.02 at. % Fe were measured under excitation with a c. w. He-Cd laser (the wavelength 442.1 nm). The spectral-slit width was equal to 0.02 nm. To study time-resolved low-temperature photoluminescence spectra for PbI_2+0.25 at. % Fe, we used a nitrogen laser (with the wavelength λ = 337.1 nm, the pulse duration 10 ns and the pulse power 5 kW) as a pulsed light source. The temperature of samples was stabilized with the accuracy 0.1 K, using an UTREKS temperature-control system.

3. Results and discussion

Crystallographic studies of the layered wide-bandgap ($E_g \approx 2.34$ eV) PbI_2 crystals have been going on for over 90 years [16]. The package of layers in lead iodide, of which thickness is approximately equal to 0.7 nm [16], consists of three atomic monolayers, I–Pb–I. In other terms, a layer of lead atoms is located between two layers of iodine atoms. The upper and lower monolayers of iodine atoms are not translationally equivalent, so that the shape of coordination polyhedron formed by iodine atoms corresponds to octahedron. Each Pb atom is surrounded by six I atoms. This forms an almost octahedral $[PbI_6]^4$ cell. Even though the basic structure of PbI_2 is simple, there are many ways of packing the elementary layers. In other words, lead iodide is characterized by a phenomenon of polytypism, which is a kind of polymorphism.

The lattice parameters of different polytypes differ only along the direction perpendicular to the layers. Lead iodide crystallizes with the formation of only hexagonal unit cell, so there are only hexagonal and rhombohedral polytypes. More than 50 PbI_2 polytypes have been identified up to now (see Ref. [17]): 2H, 4H, 6H, 30H, 6R, 12R, 36R, etc. Analyzing the previous studies [17–21], one can conclude that the symmetry of the lead iodide crystals is associated with the growth rate, the method of growth and the presence of impurities. When the PbI_2 crystals are grown from gels,

solutions and melt, a 2H polytype [17, 19] is preferably observed. It is formed by the same type of AcB layer packets. In the case of crystallization from the vapour phase, the most common are 4H and 12R polytypes [18, 20, 21]. Finally, we note that the 4H polytype contains two translationally non-equivalent layer packets AcB and CaB in its unit cell.

To determine a character of polytypes for the pure and iron-doped PbI_2 crystals grown from the vapour phase in the closed system under over-stoichiometric iodine-vapour pressure, the X-ray diffraction analysis of our samples has been performed. Fig. 1 shows the X-ray diffraction spectra for the powder samples of pure lead iodide (panel (a)) and the crystals containing 0.02 (panel (b)) and 0.25 (panel (c)) at. % of Fe. All the reflexes for the undoped crystals are associated with the 4H modification of PbI_2, in which the atomic sites are partly occupied and the space symmetry group is *P3m1*. Some of the reflexes are broadened (see Fig. 1a). In contrast to the 2H polytype (the space group $P\bar{3}m1$) and the 4H modification with fully occupied atomic sites (the space group $P6_3mc$), the theoretical reflex given by $hkl = 110$ for the 4H modification with partly occupied atomic sites is the most intense. It corresponds to the peak with the maximal intensity observed at $2\theta \approx 39.55°$ in the X-ray diffraction pattern (the case of Cu-Kα_1 radiation).

The above result is consistent with the studies conducted in Ref. [22], where the space group P3m1 for the 4H polytype of PbI_2 has been determined using the X-ray diffraction analysis on single crystals. As a result of precise studies [22] on the 2H polytype of PbI_2 crystals grown from the gel and the 4H polytype obtained by thermal transition from 2H at 423 K, it has been found that the occupation of atomic sites in the 2H and 4H structures amounts to 80–85%. The studies [21] have been performed by an ultralow-frequency Raman spectroscopy of PbI_2 plates grown by the chemical vapour deposition. The appearance of a split mode has indicated that the PbI_2 crystals

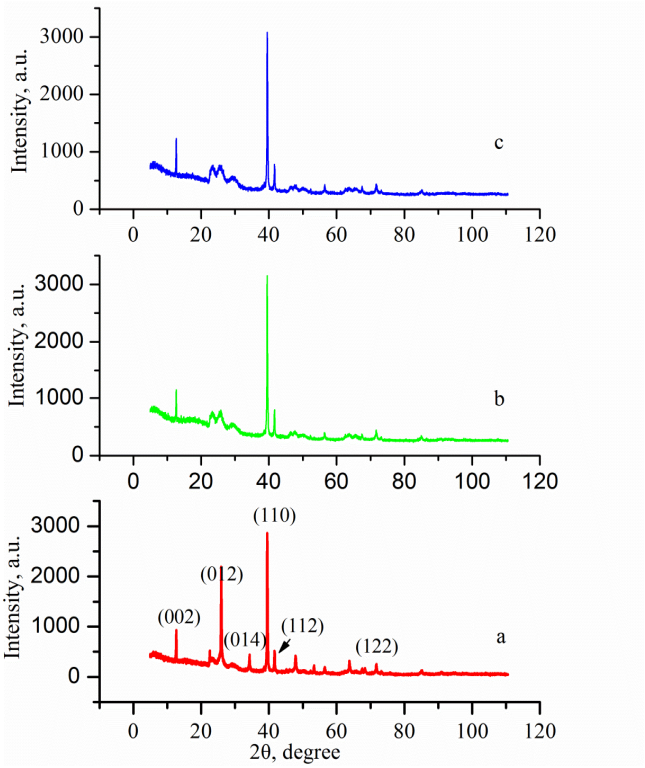

Fig. 1. X-ray diffraction patterns observed for (a) pure PbI_2, (b) PbI_2+0.02 at. % Fe, and (c) PbI_2+0.25 at. % Fe.

grown by this method correspond mainly to the 4H polytype. Such 4H structures can withstand a further process of formation of organic–inorganic perovskites [21]. Our studies confirm the fact that the 4H polytype is often formed in the samples of lead iodide grown from the vapour phase.

Fig. 1 indicates that the X-ray diffraction patterns found for lead iodide doped with iron differ from those obtained for pure PbI_2. The main differences concern the locations of the diffraction reflections and the shapes of the latter. Some of the reflexes are broadened, while the others do not appear at all. This can be due to dislocations, deformations and texturing of the samples. The X-ray diffraction spectra obtained for the samples containing 0.02 (panel (b)) and 0.25 (panel (c)) at. % of Fe are almost the same. The 4H modification of the iron-doped crystals manifests the intrinsic structural type with the space group P3m1, which is the same as for pure lead iodide. Therefore, doping of PbI_2 with iron contributes to the formation of 4H polytype, quite similar to the case of doping with Cd, Bi and Sn (see Refs. [18, 23]).

Table 1 presents the lattice parameters and the volume of the unit cell derived for the pure and iron-doped lead iodide crystals in the overall concentration range 0.01–0.25 at. % under study. The parameters obtained for the pure PbI_2 crystals agree well with those calculated in Ref. [22] (a = 4.554(1) Å, c = 13.962(5)Å, and V = 250.80(9) Å^3). Introduction of 0.01 at. % of Fe into PbI_2 increases the lattice parameters and the unit-cell volume. With a further increase in the content of the doping component (0.02–0.25 at. %), the unit-cell volume and the parameters a and c of the lattice decrease. A decrease in the unit-cell volume observed with increasing Fe content can be explained by partial replacement of Pb atoms by Fe atoms.

Table 1. Lattice parameters and unit-cell volume calculated for the PbI_2 crystals.

Fe content in the crystal, at. %	Lattice parameter a, Å	Lattice parameter c, Å	Unit-cell volume, Å^3
0	4.552	13.968	250.64
0.01	4.559	13.997	251.95
0.02	4.556	13.977	251.25
0.25	4.554	13.972	250.96

The morphologic features of our crystals (i.e., the shape, the character of surface and the degree of structural imperfection) are determined by the two factors: the nature of crystals and the conditions of their crystallization. The morphology of PbI_2 crystals doped with Fe, which are grown from the vapour phase, has earlier been studied using both optical and scanning electron microscopy techniques. When the iron iodide is introduced into the PbI_2–I_2 system, the crystals grow in the shapes of ribbons, plates, ribbon splices, and plate splices (often twins).

Fig. 2a shows a general view of our crystals: a ribbon-shaped crystal, a plate, and a twin splice. When growing the pure PbI_2 crystals from the vapour phase in the closed system under over-stoichiometric iodine-vapour pressure, one observes the morphological types listed above. In addition, needle-like crystals and elongated strips with pointed ends are also detected [24, 25]. When being doped with iron in the region 0.01, 0.02 and 0.25 at. %, the crystals have a ribbon-like shape in most cases, with the lengths 1–2.5 cm, the widths 1–4 mm and the thicknesses 0.01–0.1 mm.

As seen from Fig. 2a–d, the surface of real crystals is not perfectly smooth and contains such features as growth layers, growth steps, fractures formed by unfinished growth steps, echelons of growth steps, and sub-individuals (with outgrowths or depressions being covered with the same faces as those observed in the main crystal). The surface of the crystals gives an idea of the last stages of its formation. In particular, Fig. 2a–c shows a layered character of the growing (001)

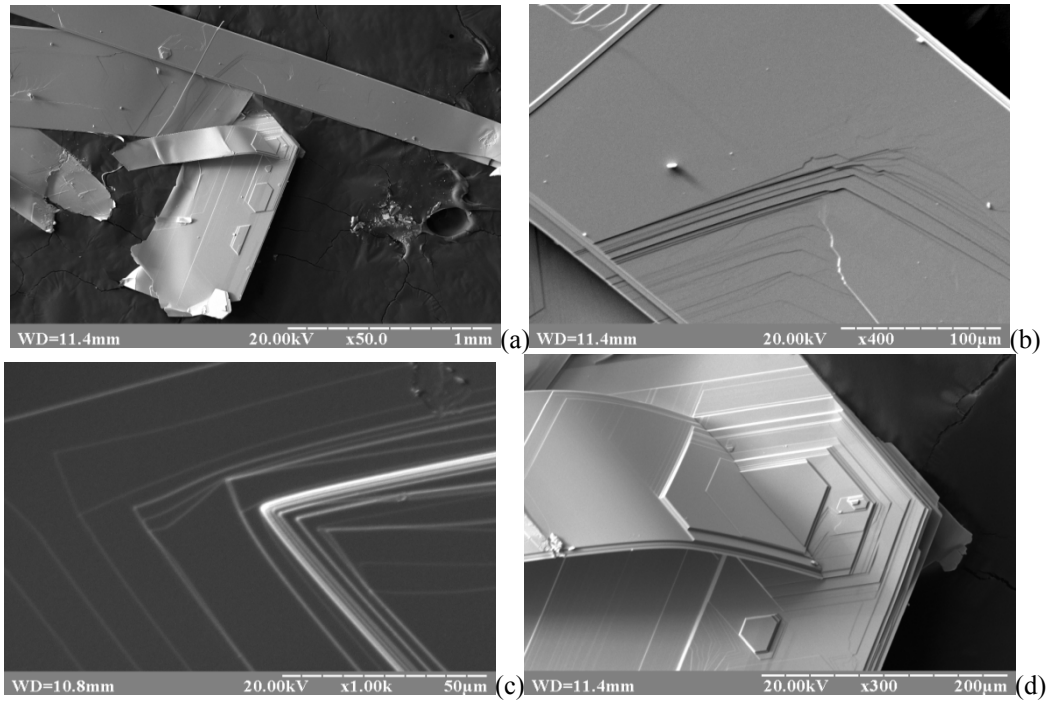

Fig. 2. Morphological features observed for the crystals PbI_2+0.02 at. % Fe: (a) a general view of crystals grown from the vapour phase, (b) a fracture, (c) layers and steps of growth, and (d) a growth twin.

faces in the shape of terraces, which is accompanied by the appearance of characteristic stepped surface relief of the crystals. Macro-terraces parallel to the crystal surface are formed due to interaction of crystallizing elementary layers. The location of steps on the surface (see Fig. 2c) can be described as follows: the greater the inclination angle, the more densely they are located. Due to release of heat during crystallization, the steps located nearby grow more slowly than the wider steps. Wide steps catch up with the groups of narrower steps and further slow down their growth rate. Layers in the shape of hexagons (see Fig. 2a, d) turn into ribbons with further growth. This can be explained by growth anisotropy: the planes that move forward along the normals with the lowest velocities grow tangentially and displace the fast-growing faces.

Fig. 2d shows a growth twin with a twinning plane in which individuals only touch each other. The formation of growth twins occurs during crystal growth and is caused by deformation of the crystal under external forces or internal stresses. When the crystals grow from the vapour phase, twinning can be caused by impurities, thermal gradients available along the crystal surface (or thermal shocks), and inhomogeneity of diffusion field [26]. Fig. 2d testifies a layered structure of the crystals. The appropriate angle, 120°, is characteristic for hexagonal crystallites, which has also been observed for the PbI_2 crystals grown by a chemical-steam transport under the condition that iodine is a self-transporting agent [27].

Low-temperature photoluminescence spectroscopy is one of the main experimental methods for studying the optical properties of semiconductor materials. Fig. 3 shows the photoluminescence spectrum measured for the crystals PbI_2+0.02 at. % Fe at the temperature 5 K. There are three emission bands in the spectrum. The band with the maximum located at about 495 nm is due to the exciton emission caused by recombination of free and bound excitons at donor centres. According to Ref. [28], the donor centre that binds the exciton is iodine vacancy, which is always present in the crystals due to strong volatility of iodine. Following the study [29],

one concludes that the main mechanism of the emission band located near 510 nm is recombination of shallow intrinsic donors and acceptors. In particular, these are spatially bound donor vacancies of iodine and acceptor vacancies of lead.

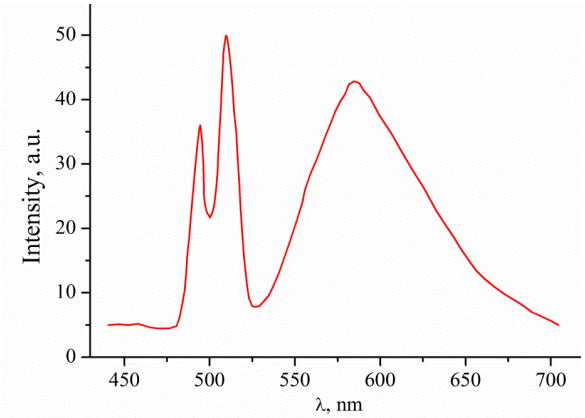

Fig. 3. Photoluminescence spectrum detected for the crystals PbI_2+0.02 at.% Fe at T = 5 K.

The third broad long-wave band with the maximum centred at about 590 nm is associated with coexistence of the two types of recombination mechanisms [29]: a 'fast' bimolecular one, which dominates at excitation inside the fundamental-absorption region and a 'slow' mechanism which dominates in the case of excitation inside the exciton band due to donor–acceptor recombination. The authors [30] have explained this band by the vacancies of lead. The spectrum presented in Fig. 3 demonstrates that introduction of 0.02 at.% iron dopant into PbI_2 gives rise to no additional emission bands.

As established in the work [13], the increase in Fe concentration from 0.001 to 0.01 at. % is accompanied by a nonlinear increase in the exciton bandwidth and a decrease in the maximal amplitude.

The study of time-resolved low-temperature (T = 4.2 K) photoluminescence spectra of PbI_2 + 0.25 at. % Fe under pulsed-laser excitation has revealed that the photoluminescence spectrum in the region of nanosecond resolutions is dominated by a high-energy emission band located at 490–500 nm. Fig. 4 presents the photoluminescence spectra of the same doped lead iodide crystals, which have been detected at the microsecond resolution. The spectral distribution of the photoluminescence intensity changes noticeably in the latter case: the spectrum is now dominated by a wide emission band located in the region 520–690 nm. With increasing iron concentration (from 0.02 to 0.25 at. %), the maximum of this low-energy band (2.0–2.4 eV) shifts towards the region of shorter wavelengths (from 590 to 560 nm – cf. Fig. 3 with Fig. 4).

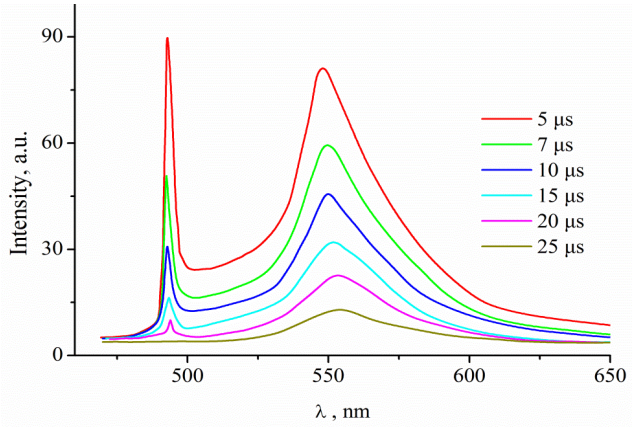

Fig. 4. Time-resolved photoluminescence spectra detected for the crystals PbI_2+0.25 at. % Fe at the temperature T = 4.2 K.

The lifetime τ of this luminescence band can be determined from the experimental decay curve, using a single-exponential fit. Namely, the lifetime value $\tau \approx 14$ μs has been obtained from the temporal dependence of the emission-band intensity plotted on a semi-logarithmic scale. Explaining the nature of the short-wavelength shift of the maximum of this band requires further studies. We only note in this relation that the experimental results and the relevant theoretical calculations do not match with each other. The energy spectrum and the spectrum of intra-centre transitions of the dopant Fe^{2+} ions have been calculated for the PbI_2 crystals [15], using a crystal-field theory and taking into account an inter-configuration interaction. The appearance of the 17210 cm^{-1} (581 nm) and 23705 cm^{-1} (422 nm) lines in the absorption spectrum has been predicted. In order to determine the effect of electron–phonon interactions and the levels of Fe dopant upon the photoluminescence spectra of PbI_2, theoretical calculations have been performed in Ref. [31], using a mixed basis constructed from linear combination of atomic orbitals and pseudo-potential wave functions. The appearance of two bands centred at the wavelengths 520 and 495 nm has been predicted [31]. Experimental investigations of the nature and specific mechanisms of the emission bands observed in the PbI_2:Fe crystals will be a subject of future work.

4. Conclusion

The PbI_2 crystals have been grown from the vapour phase. The X-ray diffraction patterns obtained for both undoped and iron-doped lead iodide (the concentration range 0.01–0.25 at. %) have been described by the 4H polytype modification in which the atomic positions are partly occupied (the space symmetry group *P3m1*). The introduction of Fe dopant with the concentration 0.01 at. % increases the lattice parameters *a* and *c*. With further increase in the dopant content up to 0.25 at. %, the volume of the unit cell decreases. Fe doping promotes the growth of lead iodide single crystals mainly in the shape of ribbons.

It has been found that, at the iron content up to 0.25 at. %, no extra emission bands are observed in the low-temperature ($T = 4.2$ K) photoluminescence spectra. The increase of iron content in the PbI_2 crystals (from 0.02 to 0.25 at. %) is accompanied by the shift of maximum of the long-wavelength emission band from 590 to 560 nm (i.e., it is located in the region 2.0–2.3 eV).

References

1. Zhu X, Sun H, Yang D, Wangyang P and Gao X, 2016. Comparison of electrical properties of X-ray detector based on PbI_2 crystal with different bias electric field configuration. J. Mater. Sci. Mater. Electron. **27**: 11798–11803.
2. Caldeira Filho A M and Mulato M, 2011. Characterization of thermally evaporated lead iodide films aimed for the detection of X-rays. Nucl. Instr. Meth. A. **636**: 82–86.
3. Lee C H, Shin Y, Jeon G, Kang D, Jung J, Jeon B, Park J, Kim J and Yoon C, 2021. Cost-efficient effect of low-quality PbI_2 purification to enhance performances of perovskite quantum dots and perovskite solar cells. Energies. **14**: 1–12.
4. Gujar T P, Under T, Schonleber A, Fried M, Panzer F, Smaalen S, Kohler A and Thelakkat M, 2018. The role of PbI_2 in $CH_3NH_3PbI_3$ perovskite stability, solar cell parameters and device degradation. Phys. Chem. Chem. Phys. **20**: 605–614.
5. Li R, Zhang H, Zhang M and Guo M, 2018. Effect of PbI_2 solution on air-preparation of perovskite solar cells for enhanced performance. Appl. Surf. Sci. **458**: 172–182.
6. Murugadoss G, Thangamuthu R, Kumar M R and Ravishankar R, 2019. Organic-free indium-doped cesium lead iodide perovskite for solar cell application. Micr. Nano Lett. **14**: 1385–1387.

7. Zhong M, Huang L, Deng H-X, Wang X, Li B, Wei Z and Li J. 2016. Flexible photodetectors based on phase dependent PbI_2 single crystals. J. Mater. Chem. C. **4**: 6492–6499.
8. Augustoa G S, Oliveirab T A, Mouraa G M, Silvaa C C, Condelesb J F, Moretob J A, Oliveiraa P R, Mulatoc M and Gelamoa R V, 2019. Development and characterization of PbI_2 nanoparticles for all solid-state flexible supercapacitor purposes. Mater. Res. **22**: 1–8.
9. Miysaka T, 2015. Perovskite photovoltaics: rare functions of organolead halide in solar cells and optoelectronic devices. Chem. Lett. 44: 720–729.
10. Pogorily A M, Ryabchenko S M and Tovstolytkin A I, 2010. Spintronics. Basic phenomena. Trends of development. Ukr. J. Phys. **6**: 37–97.
11. Rybak O V, 2019. Growth and properties of Mn-doped PbI_2 crystals. Inorg. Mater. **55**: 612–616.
12. Vertegel I G, Chesnokov E D, Ovcharenko O I, Bukivskii A P and Gnatenko Yu P, 2019. Influence of Mn^{2+} ions on parameters of the I^{127} NQR spectrum of a mixed layered $Pb_{1-x}Mn_xI_2$ semiconductor. Func. Mater. **26**: 744–747.
13. Rybak O V, Lun' Yu O, Bordun I M and Omelyan M F, 2005. Crystal growth and properties of PbI_2 doped with Fe and Ni. Inorg. Mater. **41**: 1272–1276.
14. Stolyarchuk I D, Savchuk A I, Makoviy A I, Shporta O A, Savchuk O A, Stefaniuk I and Rogalska I, 2013. Optical and magneto-optical properties of $PbFeI_2$ nanoparticles. Proc. SPIE. **9066**: 1–6.
15. Kramar AV, Kramar N K, Melnychuk S V and Melnyk P I, 2004. Intracentre absorption spectra by the 3d-group impurity ions in PbI_2. Phys. Chem. Solid State. **5**: 91–93.
16. Beckmann P A, 2010 A review of polytypism in lead iodide. Cryst. Res. Technol. **45**: 455–460.
17. Shah M A and Wahab M A, 2000. Growth rate and symmetry of polytypes in MX_2-compounds. J. Mater. Sci. Lett. **19**: 1813–1816.
18. Kaur H, 2014. Challenges in the study of polytypism in MX_2 compounds. Adv. Appl. Sci. Res. **5**: 259–261.
19. Chaudhary S K, 2012. Lead iodide crystals as input material for radiation detectors. Crystal structure theory and applications. **1:** 21–24.
20. Nakashima S, 1975. Raman study of polytypism in vapour grown PbI_2. Solid State Commun. **16**: 1059–1062.
21. Cong C, Shang J, Niu L, Wu L, Chen Y, Zou C, Feng S, Qiu Z-J, Hu L, Tian P, Liu Z, Yu T and Liu R, 2017. Anti-Stokes photoluminescence of van der Waals layered semiconductor PbI_2. Adv. Opt. Mater. **5**: 1700609.
22. Palosz B, Steurer W and Schulz H, 1990. The structure of PbI_2 polytypes 2H and 4H: a study of the 2H-4H transition. J. Phys.: Condens. Matter, **2**: 5285–5295.
23. Rybak O V, Semkiv I V and Chekailo M V, 2020. Growth and properties of Cd-doped PbI_2 crystals. J. Nano- and Electron. Phys. **12**: 01019.
24. Kurilo I V and Rybak O V, 2002. Effect of growth conditions on the morphology and structural perfection of vapor-grown PbI_2 crystals. Inorg. Mater. **38**: 288–291.
25. Rybak O V and Kurilo I V, 2002. Mass transport in the PbI_2–I_2 system. Inorg. Mater. **38**: 854–858.
26. Kozlova O G. Morphological and genetic analysis of crystals. Moscow: MGU Press, 1991 (in Russian).
27. Lin D Y, Guo B C, Dai Z Y, Lin C F and Hsu H P, 2019. PbI_2 single crystal growth and its optical property study. Crystals, **9**: 598.

28. Brodin M S, Bibik V A and Davydova N A, 1989. Phase transformations of the order-disorder-order type in layered PbI_2 crystals under the action of laser radiation. Fiz. Tverd. Tela. **31**: 117–122.
29. Derenzo S T, Bourret-Courchesne E, Yan Z, Bizarty G, Canning A and Chang G, 2013. Experimental and theoretical studies of donor-acceptor scintillation from PbI_2. J. Lumin. **134**: 28–34. doi 10.1016/j.jlumin.2012.09.022
30. Blazhkiv V S, Gamernyk R V and Grigorovich V M, 1992. Defect system in PbI_2 crystals. Ukr. Fiz. Zhurn. **37**: 425–428.
31. Rybak O, Blonskii I V, Bilyi Ja M, Lun Yu, Makowska-Janusik M, Kasperczyk J, Berdowski J, Kityk I V and Sahraoui B, 1998. Luminescent spectra of PbI_2 single crystals doped by 3d-metal impurities. J. Lumin. **79**: 257–267.

Rybak O. V. and Chekaylo M. V. 2021. Structural, morphological and luminescence studies of Fe-doped PbI_2 crystals. Ukr.J.Phys.Opt. **22**: 270 – 278. doi: 10.3116/16091833/22/4/270/2021

Анотація. *Наведено результати рентгеноструктурних досліджень нелегованих і легованих Fe монокристалів йодиду свинцю у діапазоні концентрацій 0,01–0,25 ат. %. Кристали PbI_2 і PbI_2:Fe одержано кристалізацією з парової фази в закритій системі під надстехіометричним тиском парів йоду. Морфологію цих кристалів проаналізовано за допомогою скануючого електронного мікроскопа. З'ясовано вплив легування залізом на низькотемпературні (T = 4,2 K) спектри фотолюмінесценції йодиду свинцю.*